U.S. Department
of Transportation
National Highway
Traffic Safety
Administration

NHTSA

DOT HS 813 540c

May 2024

Restraint Design for Obese Occupants: Belt Pull Test Simulations Error Effects Modeling

Page intentionally left blank.

DISCLAIMER

This publication is distributed by the U.S. Department of Transportation, National Highway Traffic Safety Administration, in the interest of information exchange. The opinions, findings, and conclusions expressed in this publication are those of the authors and not necessarily those of the Department of Transportation or the National Highway Traffic Safety Administration. The United States Government assumes no liability for its contents or use thereof. If trade or manufacturers' names or products are mentioned, it is because they are considered essential to the object of the publication and should not be construed as an endorsement. The United States Government does not endorse products or manufacturers.

NOTE: This report is published in the interest of advancing motor vehicle safety research. While the report may provide results from research or tests using specifically identified motor vehicle models, it is not intended to make conclusions about the safety performance or safety compliance of those motor vehicles, and no such conclusions should be drawn.

Suggested APA Format Citation:

Sun, Z., Kerrigan, J. R., Joodaki, H., & Gepner, B. (2024, May). *Restraint design for obese occupants: Belt pull test simulations error effects modeling* (Third of four parts. Report No. DOT HS 813 540c). National Highway Traffic Safety Administration.

The other three parts of this series:

Joodaki, H., Gepner, B., & Kerrigan, J. R. (2024, May). *Restraint design for obese occupants* (First of four parts. Report No. DOT HS 813 540a). National Highway Traffic Safety Administration.

Kerrigan, J. R., Joodaki, H., Sun, Z., & Gepner, B. (2024, May). *Restraint design for obese occupants: Rear-seat simulations* (Second of four parts. Report No. DOT HS 813 540b). National Highway Traffic Safety Administration.

Kerrigan, J. R., Forman, J., Gepner, B., Joodaki, H., & Sun, Z. (2024, May). *Restraint design for obese occupants: Obese GHBMC model modifications* (Fourth of four parts. Report No. DOT HS 813 540d). National Highway Traffic Safety Administration.

Page intentionally left blank.

Technical Report Documentation Page

1. Report No.	2. Government Accession No.	3. Recipient's Catalog No.
DOT HS 813 540c		

4. Title and Subtitle	5. Report Date
Restraint Design for Obese Occupants: Belt Pull Test Simulations Error Effects Modeling (Third of four parts)	May 2024
	6. Performing Organization Code
7. Authors	8. Performing Organization Report No.
Zhaonan Sun, Jason R. Kerrigan, Hamed Joodaki, Bronek Gepner	
9. Performing Organization Name and Address	10. Work Unit No. (TRAIS)
University of Virginia Center of Applied Biomechanics 4040 Lewis and Clark Dr. Charlottesville, VA 22911	11. Contract or Grant No. DTNH2215D00022
12. Sponsoring Agency Name and Address	13. Type of Report and Period Covered
National Highway Traffic Safety Administration 1200 New Jersey Avenue SE Washington, DC 20590	. 14. Sponsoring Agency Code

15. Supplementary Notes

16. Abstract

Third of four parts. This task evaluates the Global Human Body Models Consortium (GHBMC) models representing obese people with respect to the obese postmortem human surrogates test series of tabletop belt pull tests previously performed at the University of Virginia's Center for Applied Biomechanics. Using a finite element model of the test fixtures, 3D drawings of the original test fixtures were obtained and meshed. To investigate whether the GHBMC obesity model can show kinematics like the PMHS, additional sensitivity studies were performed. The results showed that none of the implemented changes could lead the GHBMC obesity model to submarining.

17. Key Words	18. Distribution Statement
GHBMC, finite element, model, obese, Global Human Body Models Consortium	This document is available to the public from the DOT, BTS, National Transportation Library, Repository & Open Science Access Portal, https://rosap.ntl.bts.gov.

19. Security Classif. (of this report)	20. Security Classif. (of this page)	21. No. of Pages	22. Price
Unclassified	Unclassified	48	

Form DOT F 1700.7 (8-72) Reproduction of completed page authorized

Page intentionally left blank.

Table of Contents

List of Figures

List of Tables

Executive Summary

The aim of this study was to evaluate the Global Human Body Models Consortium (GHBMC) obesity models with respect to the obese postmortem human surrogates (PMHS) test series of tabletop belt pull tests previously performed at the University of Virginia's Center for Applied Biomechanics. Simulation results of the GHBMC model of obese males who had a stature of 1,750 mm, a weight of 86 kg and a body mass index (BMI) of 30 were compared to the response of the female PMHS with a BMI of 31.0, height of 1,650 mm and weight of 84.4 kg.

The finite element model (FEM) of the test fixtures used in the belt pull tests was developed prior to any simulations. 3D drawings of the original test fixtures were obtained and meshed. All parts were modeled as rigid bodies. The GHBMC obesity model was positioned according to the initial position of the PMHS. A seat belt was fitted to the GHBMC model, and a series of simulations were conducted to compare the model response with the PMHS.

In several loading conditions the PMHS showed substantial belt shearing on the abdominal flesh, resulting in the lap belt sliding over the pelvis and pulling directly into the abdomen. In this study, we defined this motion as submarining. However, the GHBMC obesity models did not show similar kinematics under corresponding loading conditions. Instead, the lap belt engaged well with the pelvic wings, leading to no shearing of the abdominal flesh, and prevented the belt from sliding into the abdomen.

To investigate whether the GHBMC obesity model can show kinematics like the PMHS, additional sensitivity studies were performed. First, belt position relative to the pelvic wings was changed to explore the effect of belt position on the pelvis engagement. Second, the load limit was changed. Third, extreme pulling directions not in the PMHS tests were simulated to explore their effects. In addition, the effects of abdominal organs were studied by removing all abdominal organs. Last, the material properties of the flesh were modified, and alternative material models were studied.

The results showed that none of the implemented changes could lead the GHBMC obesity model to submarining. The lap belt engaged well with the pelvic wings in all cases. The motion of the lap belt always aligned with the pulling direction and with no observed shearing response. However, it was found that, if a material model with low shear stiffness was used, the belt tended to shear, but proved to be unstable due to the current formulation. It showed that changing the material properties as well as the formulation could potentially lead to a stable model capable of simulating occupant submarining. Finally, several of these findings were further published in peer reviewed publications (Gepner et al., 2018; Sun, Gepner, & Kerrigan, 2019).

Page intentionally left blank.

Summary of Findings

Overall, no simulation demonstrated the belt-slip-over-pelvis kinematics that were observed in the cadaveric testing. Specifically, several conclusions can be made based on the results of the belt pull test simulations.

1. Model positioning has little to no effect on lap belt kinematics and resultant force.
2. Increasing lap belt load limit leads to an increase in belt penetration depth while belt displacement direction remained unchanged. No shear motion was observed with an increased belt pull force.
3. Changing belt position has not led to shear motion over the pelvis into the abdomen.
4. Abdominal organs provided additional compressive stiffness beyond what was provided by abdominal flesh. Removing abdominal organs resulted in larger belt penetration, but the belt kinematics remained unchanged.
5. Direction of belt motion was aligned with belt-pulling direction despite pulling angle changes. No shearing motion was observed.
6. Abdominal flesh in the obese GHBMC appeared to be orders of magnitude stiffer in shear compared to subcutaneous adipose tissue. Changing material models to make shear stiffness lower did not result in shear motion in the abdominal region.

Page intentionally left blank.

GHBMC Obesity Models Introduction

This section provides an overview of the 12 morphed human models based on GHBMC M50-O v4.4 developed by the University of Michigan Transportation Research Institute (2017). The reference anthropometric values of the GHBMC M50-O as well as the morphed human models are shown in Table 1, which represent a wide range of age and body shapes. Figure 1 shows the sectional view of all 12 morphed human models.

Table 1. Anthropometries of the GHBMC obesity models

Subject #	Age (YO)	Stature (cm)	Sex	Target Weight (kg)	Target BMI (kg/m²)	Model Weight (kg)	Model BMI (kg/m²)
GHBMC M50-O	26 or older	174.9	M	78.62	25.7	77.01	25.17
1	30	175	M	76.56	25	72.73	23.75
2	30	175	M	91.88	30	85.95	28.07
3	30	175	M	107.19	35	101.25	33.06
4	30	188	M	88.36	25	84.31	23.85
5	30	188	M	106.03	30	99.14	28.05
6	30	188	M	123.7	35	115.89	32.79
7	70	175	M	76.56	25	74.69	24.39
8	70	175	M	91.88	30	87.39	28.54
9	70	175	M	107.19	35	103.04	33.65
10	70	188	M	88.36	25	86.32	24.42
11	70	188	M	106.03	30	100.94	28.56
12	70	188	M	123.7	35	118.01	33.39

The process for morphing the GHBMC M50-O model into occupants with different stature and body shape began with statistical skeleton models, including ribcage, pelvis, femur, and tibia, along with external body shape models of human geometry that describe morphological variations within the population as functions of overall parameters (typically age, sex, stature, and BMI). Mesh morphing methods were used to rapidly morph the GHBMC M50-O model into target geometries. In all the morphed models, material properties were not changed. In other words, only the geometrical variations were considered in the morphed models, but not the material property variations (UMTRI, 2017).

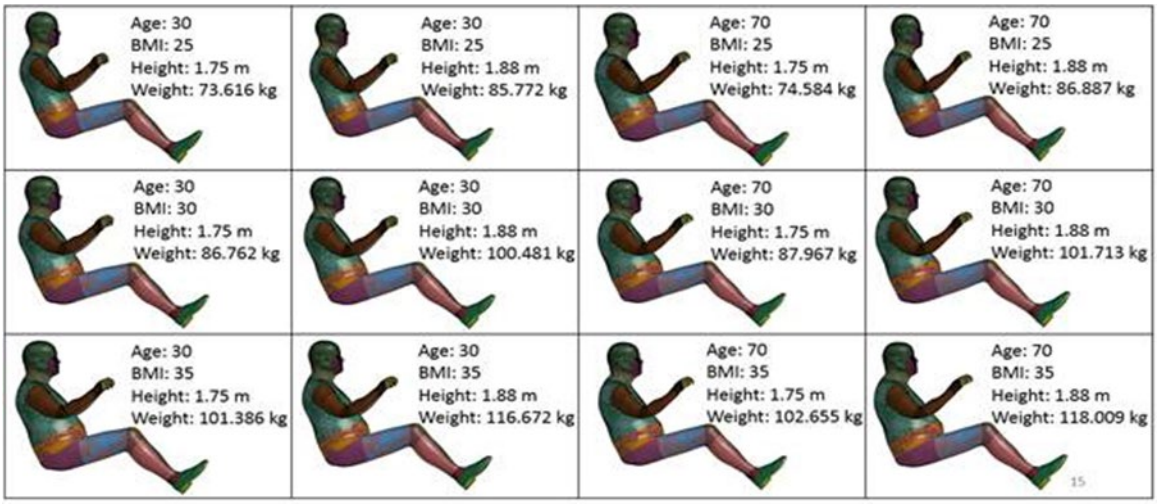

Figure 1. Anthropometries of the GHBMC obesity models

Page intentionally left blank.

Modeling of the Belt Pull Test

Belt Pull Test Introduction

Belt pull test simulation was based on a series of PMHS tests conducted at the University of Virginia's Center for Applied Biomechanics (Kim, Forman,et al., 2014; Kim, Lee, et al., 2015). The goal of the test was to generate biomechanical responses of the PMHSs under lap belt loading conditions. In the PMHS test chosen for comparison with the model, the spines of the subject were rigidly mounted to a test fixture through a mounting system to minimize the influence of the spinal motion during the test. The pelvis of the subject was positioned close to the normal driving posture, but the torso angle was more reclined than the average driving posture due to the difficulty of adjusting the torso angle during the mounting process. This torso angle led to the belt being positioned more rearward (or anterior) with respect to the anterior superior iliac spine (ASIS) in the longitudinal direction. Two force limits, 1 and 3 kN, were used for lap and shoulder belt tests. The applied boundary conditions were documented for the purpose of future studies. During the lap belt tests, both submarining and no submarining like belt kinematics, and a large amount of abdominal compression was observed during the submarining cases. The main outcomes from this test series were: 1) identification of compliance (belt displacement vs. belt force) of the abdominal area, 2) quantification of skin motion relative to bones under belt loading conditions, and 3) recorded detailed information on boundary conditions. The test data generated through the belt pull test was used for comparison with the GHBMC obesity models. It was decided that this step was necessary prior to using the obese models in the proposed parametric study or optimization, which could identify submarining conditions and evaluate effects of countermeasures for submarining.

Modeling of the Test Fixture

The test rig was modeled following the drawing and a description obtained from the previous PMHS test series. The test rig consisted of a seat and seat back to support a test subject and belt pull system, which pulls the belt at various initial stroke rates. In the tests the distance between the seat and seat back was adjustable to accommodate subjects of different sizes, and the height of anchors (or belt pulleys) was also adjustable to accommodate various belt angles. A custom rigidized belt, which was reinforced by nylon fibers, was used to minimize belt elongation. The use of a rigidized belt simplifies the comparison between the test data and the simulation results for the morphed human model validation by minimizing the belt elongation. The belt cables were connected at the ends of the belts, and load cells were installed in the belt cable to measure the belt pulling force (Figure 2). The ends of the belt were connected to steel belt cables. The belt cables were pulled by a pneumatic cylinder in rates of up to 5 m/s to mimic a typical pretensioner. This stroke rate is equivalent to up to 10 m/s if we consider it as a pretensioner, which pulls one of the belt ends.

The test fixture was modeled using the geometry from the original 3D computer-aided design (CAD) drawing (Figure 3). The following parts were created for assembly, including base frame, piston, anchor, pulling cable, seat belt, D ring, seat frame, lower spine plate, upper spine plate, spine mounts, and seat plate. Load cells were modeled as cross section outputs according to their positions in the test (Figure 4). Of these parts, all metal fixtures were modeled as rigid bodies using shell elements. Pulling cables were modeled using 1D seat belt elements. The seat belt was modeled as 2D shell elements with fabric material formulation (Figure 5).

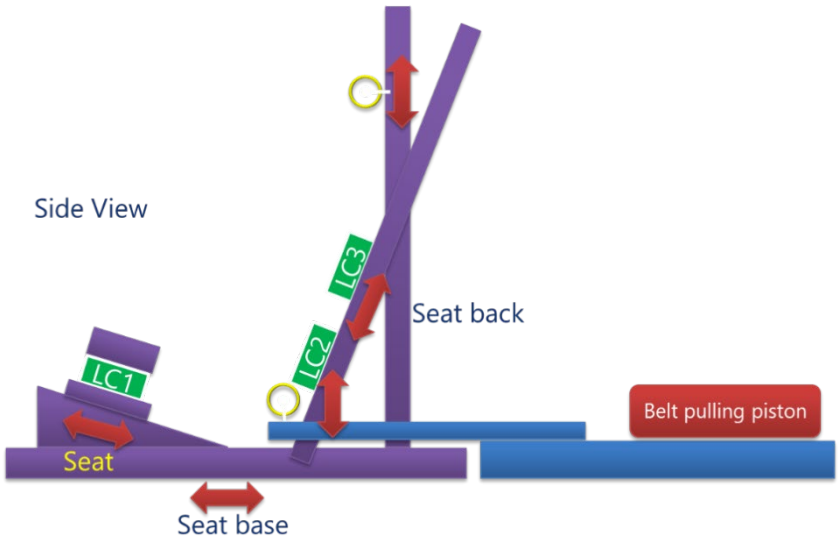

Figure 2. Schematic of the test fixture

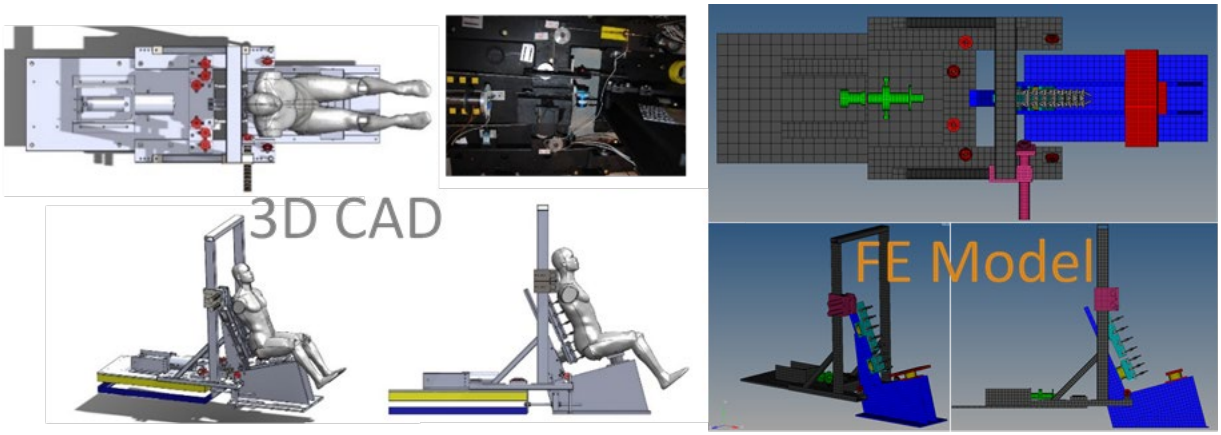

Figure 3. 3D CAD drawing of test fixture and FEM created

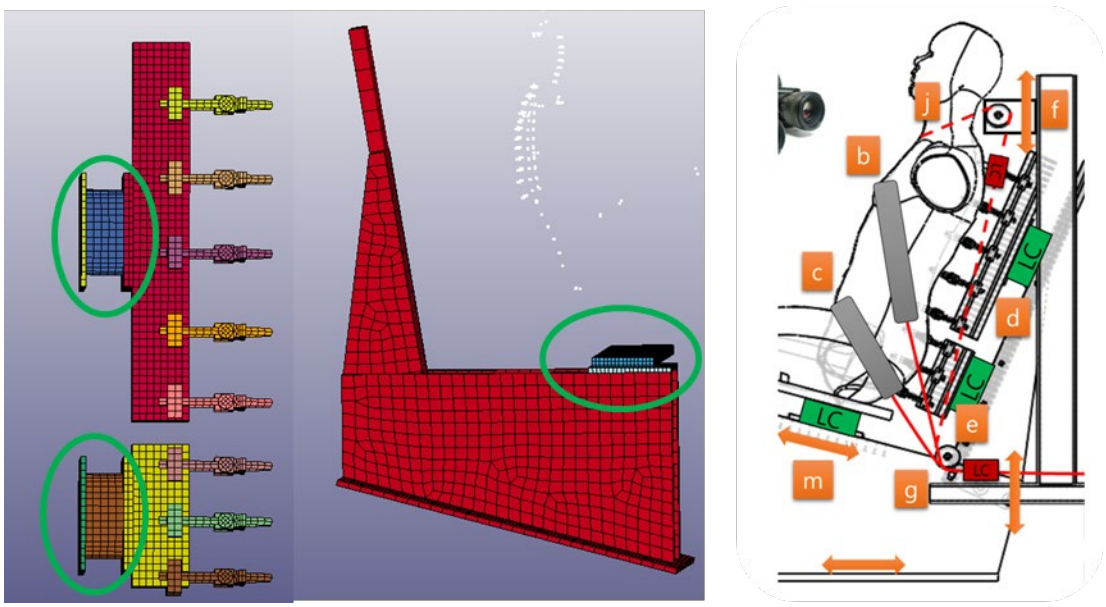

Figure 4. Load cell modeling in FEM and its position in the test

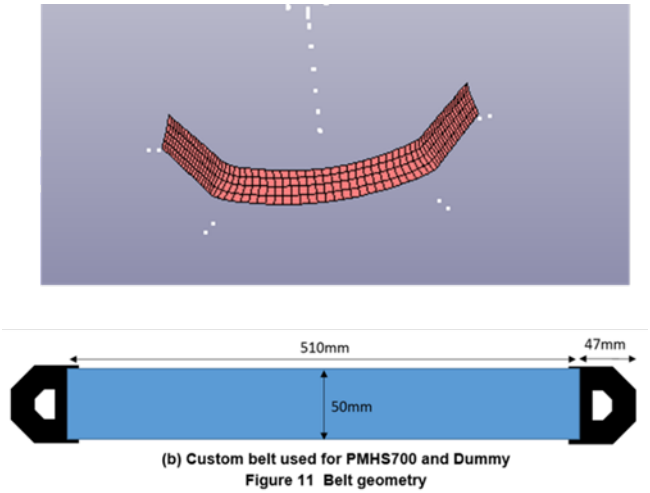

Figure 5. Schematic of custom belt used in the test and FEM

The belt pulling system was modeled using a rigid belt pulling piston, seat belt 1D and 2D elements and slip ring elements. Pulling cables modeled as 1D seat belt elements were routed through the slip ring elements (Figure 6). Additional mass elements were added to the belt to compensate for additional hardware installed in the test series. A total of 90 g was added to the model to account for the weight of the belt, clamps, bolts, and pins in the experiment (Table 2). Cable loads were extracted from the model using the cross-section force output.

Table 2. Mass compensation to the seat belt FEM

Mass [g]	PMHS700
Belt	38
Clamps	33
Bolts on clamps	6
Pins for the hole at belt ends	13
Mass of belt load cell (each)	83
Belt total (exc. load cell)	90

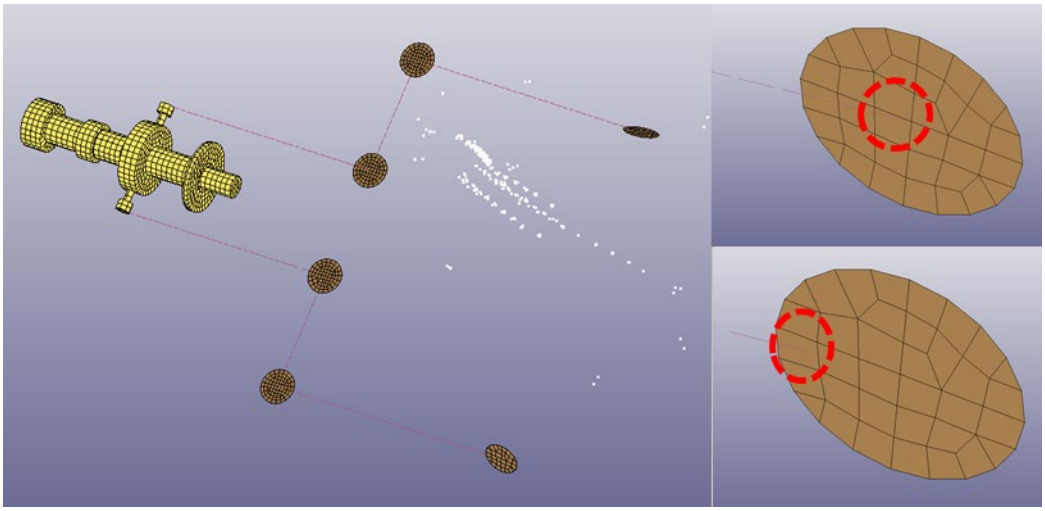

Figure 6. FEM of the pulley system for belt pulling

Test Setup

The response of the subject during the belt pull test was measured using various instrumentation, which included load cells, displacement sensors, 3D motion-tracking system, and high-speed x-ray. The belt pulling force was limited using a force limiting device by placing honeycomb between the piston disk and belt pulling disk (Figure 7). To document the boundary conditions during the test, the reaction force and moment between the subject and test rig, seat bottom and backs, were measured using multi-axial load cells (Figure 4). To characterize load distributions along the seat back, the seat back was split into two separate sections with two load cells (Figure 4). Using the Aramis optical displacement and strain mapping system determined the detailed kinematics of the belt during testing. Lastly, a high-speed x-ray system was used to record relative motion between the belt and pelvis in the sagittal plane during the lap belt test.

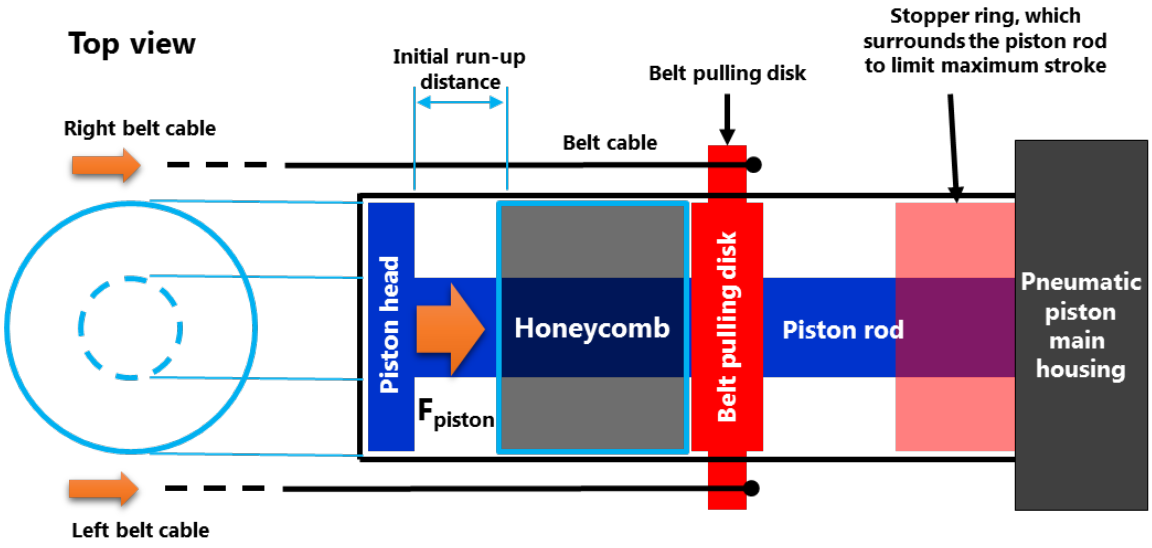

Figure 7. Load limiting device

Spine mounts (Figure 8) were installed to every other vertebra (Figure 10), and the spine mounts were attached to upper and lower spine mount columns, which were attached to the seat back of test rig through six-axis load cells (Figure 9). The spine mounts had 2° of freedom to adjust the posture of the subject, and firmly tightened after the positioning. The thoracic vertebres were mounted to the upper spine mount column and the lumbar spine and sacrum were mounted to the lower spine mount column. In PMHS700, the mounted vertebra were T1, T4, T7, T9, T11, L1, L3, L5 and sacrum (Figure 10).

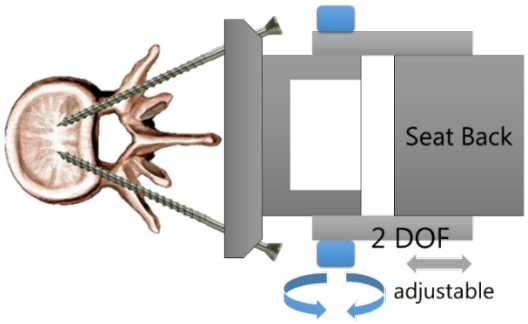

Figure 8. Spine mount (top view)

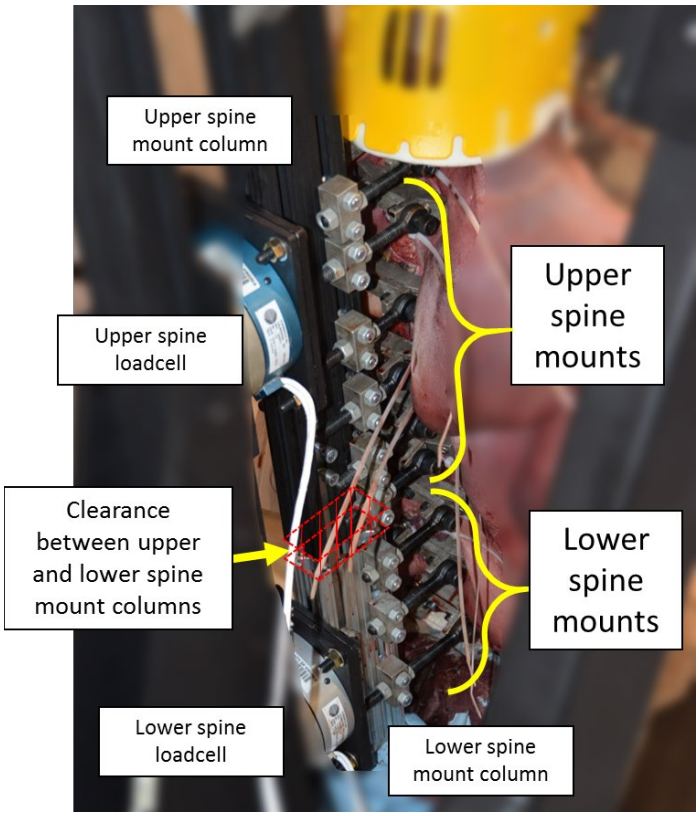

Figure 9. Subject mounted on the test rig through seat back column with spine mount

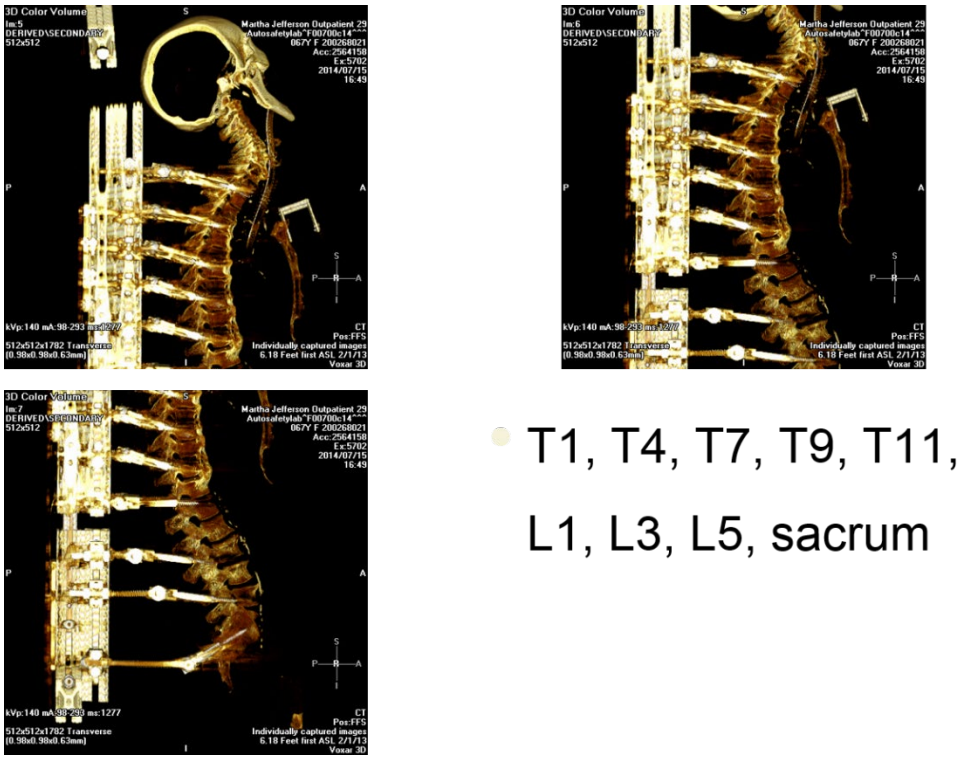

Figure 10. Spine fixation of PMHS700 in the belt pull test

Boundary Conditions

The boundary conditions were determined according to the test setup. To best match the boundary conditions of the PMHS tests the corresponding vertebra (T1, T4, T7, T9, T11, L1, L3, L5 and sacrum) were rigidly constrained in the model (Figure 11).

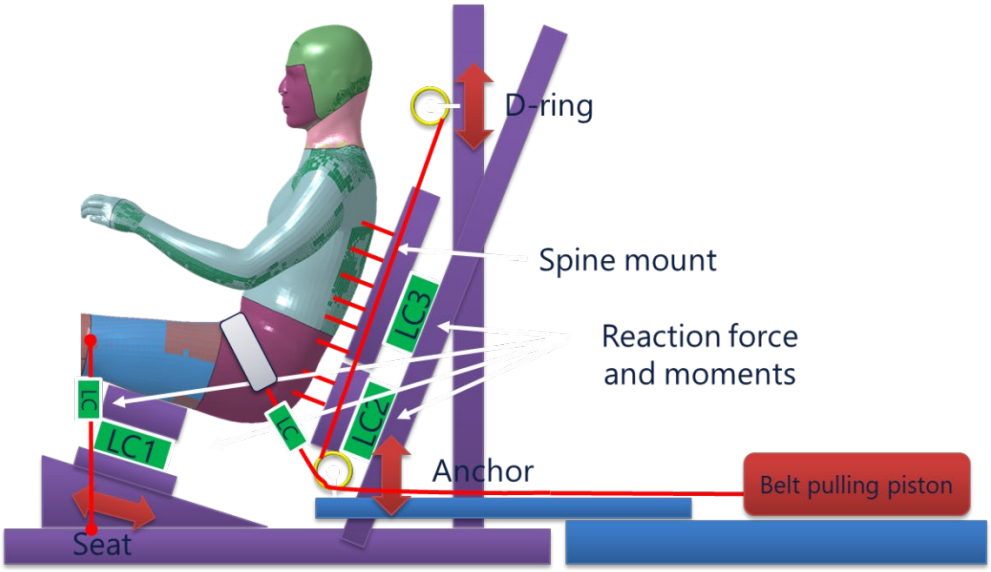

Figure 11. Boundary conditions in the test and simulation

Test Matrix

Table 3 shows the test matrix for PMHS700. The effects of different lap belt configuration as well as load limit and initial loading rate were studied in the tests.

Table 3. Test matrix of the belt pull test

Belt position	**Belt upper edge position w.r.t ASIS (X, Z), belt cable angles**	**Load limit (initial loading rate)**	**run#**
Lap belt – high angle	(-12, -53) mm, 45°	1 kN (2 m/s)	3
	(-16, -55) mm, 45°	3 kN (4 m/s)	4
	(-46, -66) mm, 45°	1 kN (2 m/s)	5
	(-35, -69) mm, 45°	3 kN (4 m/s)	6
	(-64, -82) mm, 46°	1 kN (2 m/s)	7
	(-69, -84) mm, 48°	1 kN (4 m/s)	8
Lap belt – low angle	(-70, -88) mm, 30°	1 kN (4 m/s)	9
	(-67, -84) mm, 30°	1 kN (2 m/s)	10

Test Subjects and Models

Two PMHSs, PMHS683 and PMHS700, were tested in the belt pull test. Since PMHS683 was not obese, PMHS700 was chosen as the reference for comparison. PMHS700 was a 67-year-old female with a height of 1,650 mm, weight of 84.4kg and BMI of 31.0. To minimize the differences between the PMHS and the GHBMC obesity model, the BMI 30 GHBMC obesity model with a height of 1,750 mm were chosen (Figure 12). It should be noted that all the GHBMC obesity models were males, whereas the tested PMHS were female.

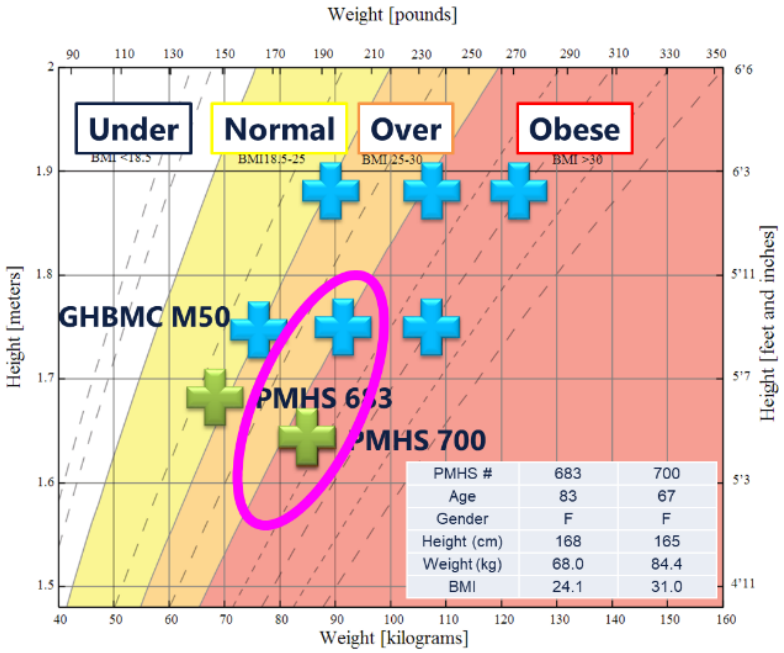

Figure 12. Anthropometry distribution of GHBMC obesity models and the PMHSs in the belt pull test

Inputs and Outputs

A force-controlled loading piston was modeled and connected to the pulling cable. The exact force time history from the corresponding PMHS tests was used as input. Recorded outputs included belt kinematics, belt cable displacements, and reaction forces from the load cells. A sample input for PMHS700-7 is shown in Figure 13.

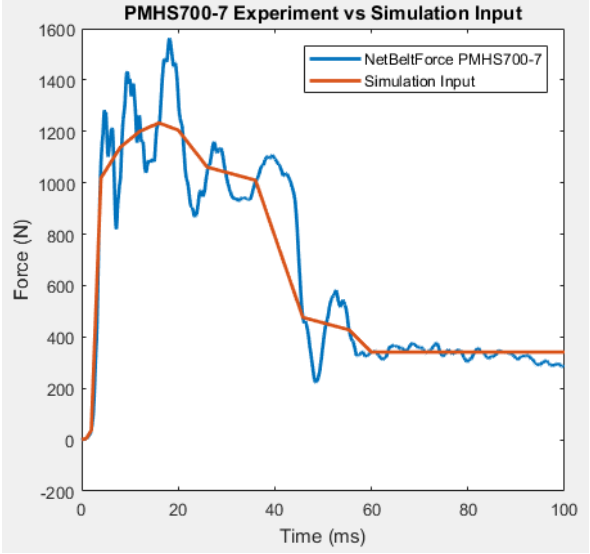

Figure 13. Input of the simulation and belt pull test

Obese GHBMC Model Positioning

Model positioning was done in two separate steps. The first step involved rigid body translation and rotation while the second step is essentially a pre-simulation that adjusts the sitting position of the model.

In the first step, information from the coordinate measuring machine, Romer Arm, and CT (computed tomography) scan were used. The goal of this step was to match the pelvis angle, defined by the ASIS and pubic symphysis in the sagittal plane. In the case of the PMHS700, this angle was set at 37°. 3D reconstruction that includes the pelvis, the whole spine and part of the test fixture was used to match this angle and a measurement of this angle was performed to check the position. Figure 14 shows the 3D reconstructed complex and modeled test fixture. End points on the spine fixation plate were used as a reference to match the scanned and modeled test fixtures.

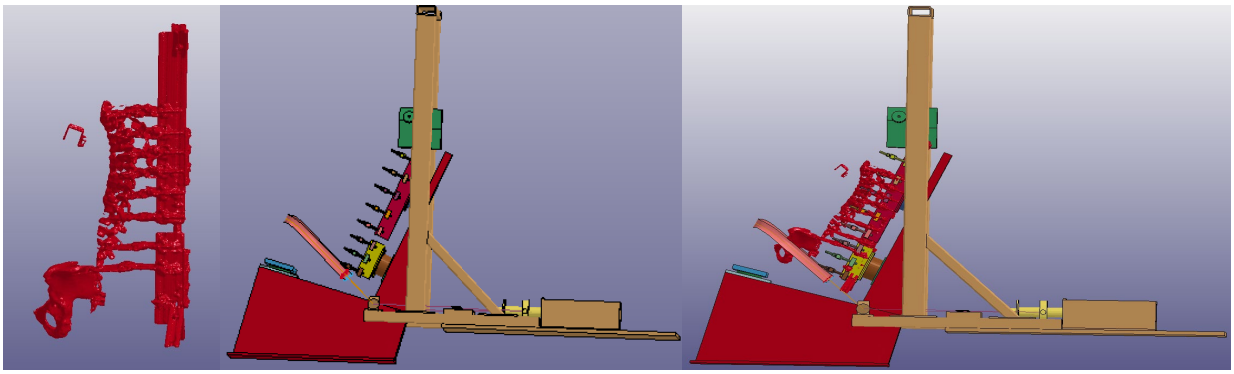

Figure 14. Rigid body translation to determine the target position of the model pelvis and spine

This translation determined the relative position of the model pelvis to the modeled test fixture. Another transformation matrix was developed to match the GHBMC obesity model pelvis to its target position. Specifically, the goal was to match the pelvis angle of the model pelvis through rigid body rotation despite the difference in pelvis geometry between the model and PMHS.

Since GHBMC and PMHS pelves had different width, a pelvic plane, a unified measure of pelvic orientation was established. The pelvic plane was defined by using the points on ASISL, ASISR and the pubic symphysis. With pelvic planes defined for both pelves, a midpoint between the ASISL and ASISR was used as an anchor point and pelvic plane normal vector as a target for pelvis orientation.

Performing a rigid body transformation resulted in the pelvis alignment shown in Figure 15. Even though both pelves were aligned as described above, a large discrepancy was observed between the lumbar spine angles in both subjects. To mitigate this, a second model was created by altering the pelvis position to match the lumbar spine angles. Since only the pelvis and lumbar alignment were used to position the second model, it was expected that the thoracic spine would require additional alignment to match the registered scan. To address this, a pre simulation was performed to reposition the model. Specifically, beam-cable elements were created to guide each vertebrae of the model to the target position defined from the PMHS tests. All vertebraes were pulled simultaneously to the target position using a force-controlled simulation. Nodal coordinates of the model were captured at the final location and used as a basis for a third initial position of the model. It should be noted that, considering the anthropometry differences between the PMHS and the model, a complete vertebra-by-vertebra match was impossible.

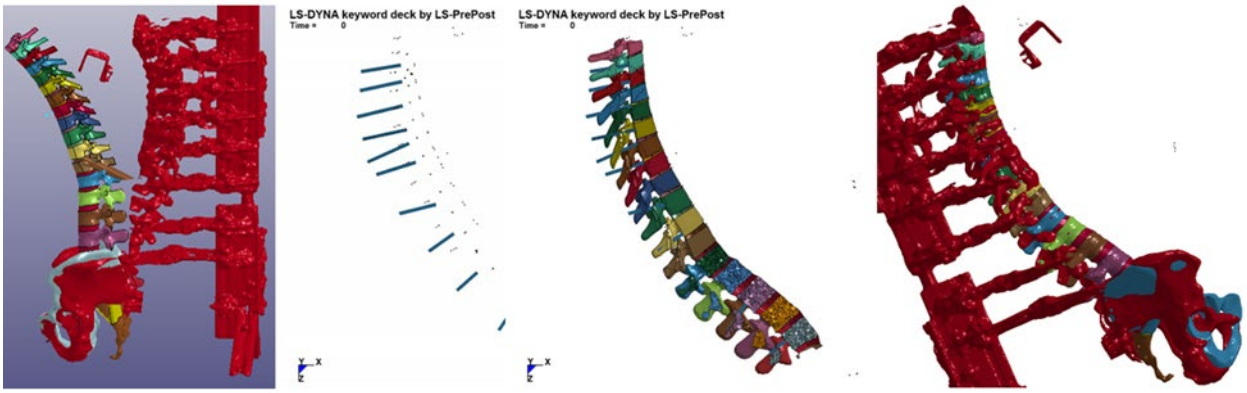

Figure 15. Pre-simulation pulls the mode spine to target position

Since the GHBMC model and target PMHS differed in anthropometry, it was not possible to match both the pelvis and spine positions to the PMHS targets at the same time. To understand the effects of pelvis and spine positioning, a sensitivity study was performed for all three different models described previously. The first model matched the pelvis angle between the two ASIS and pubic symphysis. The second model featured a rotated pelvis and matching lumbar spine angle. The third model was based on the second one, with an additional alignment of the thoracic spine to match the target PMHS.

After preparation of the three versions of the positioned model, a pilot study matching input and boundary conditions of the PMHS700-7 test was performed. The belt was positioned so that the belt angle was 46°. The test featured a 2 m/s belt pull rate and the load limit of 1 kN. The test conditions were imposed onto the models by using the experimental force time history. The belt displacement and kinematics were used as an output (Figure 16).

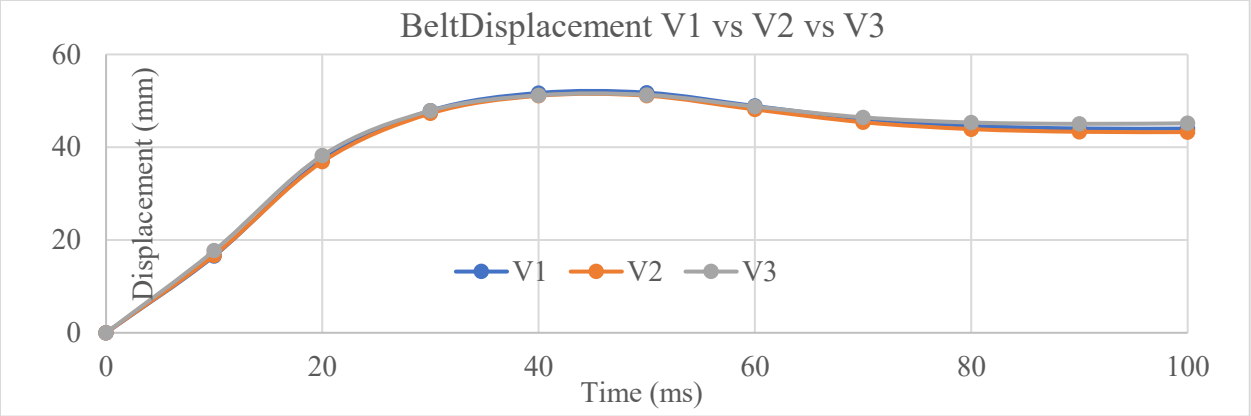

Figure 16. Belt displacements of sensitivity study of model positioning

Belt kinematics were similar in all three cases. No shearing motion of the belt was observed. The direction of belt movement was aligned with the belt-pulling direction at all times. Under the same force input, the time histories of belt displacement were similar in all three cases. No phase shifts were observed. Maximum difference among all three curves at any given moment was less than 1 mm. Based on these observations, it was concluded that the initial position of the subject had a small effect on belt displacement. For consistency, in this study, the third, prepositioned model was used for all the following evaluations.

Page intentionally left blank.

Obese GHBMC Model Evaluation

Simulation Matrix

Table 4 shows a summary of all simulations performed in this part of Task 1.

Table 4. Simulation matrix of the GHBMC obesity model evaluation

Run Number	Type	Control	Model	Referenced PMHS Test	Termination
1	Pilot Run	Displacement	M50	N/A	Error
2	Pilot Run	Displacement	1880-35M	N/A	Normal
3	Run Time	N/A	1750-35M	Kroell Thoracic Impact	Normal
4	Run Time	N/A	1880-35M	Kroell Thoracic Impact	Normal
5-7	Model Positioning	Force	1880-35M; 1750-30M	PMHS700 Initial Position	Normal
8	Baseline	Force	1750-30M	PMHS700-4	Normal
9-14	Sensitivity-Model Positioning	Force	1880-35M; 1750-30M	PMHS700-7	Normal
15-18	Sensitivity-Load Limit	Force	1750-30M	PMHS700-4 and PMHS700-8	Normal
19-23	Sensitivity-Belt Positioning	Force	1750-30M	PMHS700-3 and PMHS700-7	Normal
24-25	Abdominal Organ Effects	Force	1750-30M	PMHS700-7	Normal
26-29	Effects of Pulling Angle	Force	1750-30M	PMHS700-7	Normal
30-36	Abdominal Flesh Material Study	Force	1750-30M	PMHS700-7	Normal

Pilot Run

A pilot run (Figure 17) was performed to evaluate the stability and general behavior of the GHBMC obesity model. As a comparison, the same input and boundary conditions were applied to the 50th percentile male GHBMC model as well.

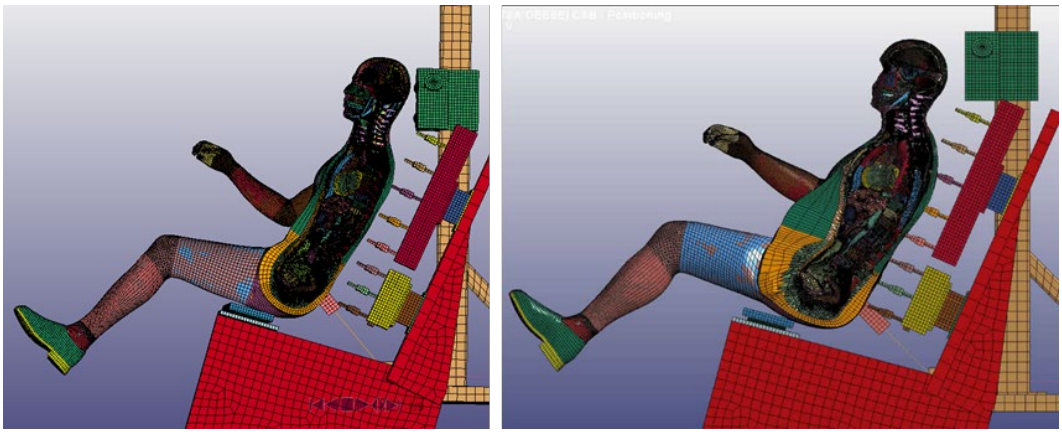

Figure 17. Pilot run of the GHBMC obesity model and AM50 model

It was found that element failure due to element distortion/negative volume occurred before the completion of the simulation in the AM50 case while the obese model reached completion. Both the GHBMC obesity model and AM50 were stiffer than the PMHS since higher belt reaction forces were observed under the same belt displacement time history. The obese model showed no submarining.

Run Time Evaluation

Two Kroell tests (Figure 18) were performed on the model representing a 30-year-old, 1,880 mm heigh, BMI 35 male and a model representing a 30-year-old, 1,750 mm height, and BMI 30 male to evaluate the stability and run time of the models. All simulations were performed using mpp LS-Dyna code and 20 processors on the InfiniBand interconnected cluster. Elapsed time for BMI 35 and BMI 30 models were 61,515 and 55,058 seconds. These times were comparable to that of a 50th percentile male GHBMC model. The GHBMC obesity model did not lead to longer run times than the 50th percentile GHBMC model.

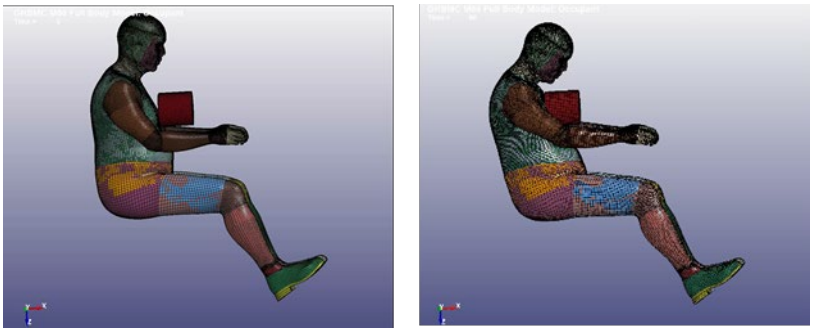

Figure 18. Run time evaluation of the GHBMC obesity model

Sensitivity on Belt Positioning

Due to large differences in abdomen shape between the PMHS and the model, a sensitivity study of belt position was performed. In the case of the PMHS, due to the smaller adipose tissue deposits around the abdomen, the upper edge of the belt was positioned above and behind the ASIS (Table 3). However similar belt position was not achievable in the case of the obese FEM, due to its larger abdomen. One of the possibilities for positioning the belt was to extract the

direction of the vector between the ASIS and the top edge of the belt from the PMHS and use it to project the top edge of the belt onto the obese FEM. However, this solution was not feasible because it would project the belt onto the chest of the obese FEM (Figure 19)

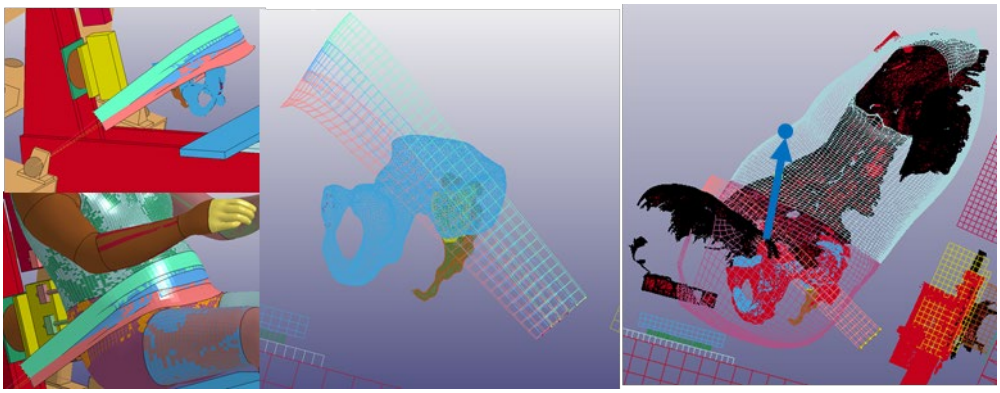

Figure 19. Belt positions used in the sensitivity study

As a result, three more realistic cases were simulated. The low position of the belt was determined by placing the lap belt as low as possible, with the lower edge of the belt in contact with the occupant lap. Next the belt was raised by a distance equal to two thirds the belt width to create the mid belt. The mid belt was then elevated to the same distance to create the high belt. It is worth noting that the low belt had its upper edge at ASIS while the high belt has a lower edge that was right above the ASIS (Figure 19). It was assumed that the response of these two would be different if the pelvis engagement played an important role in this simulation.

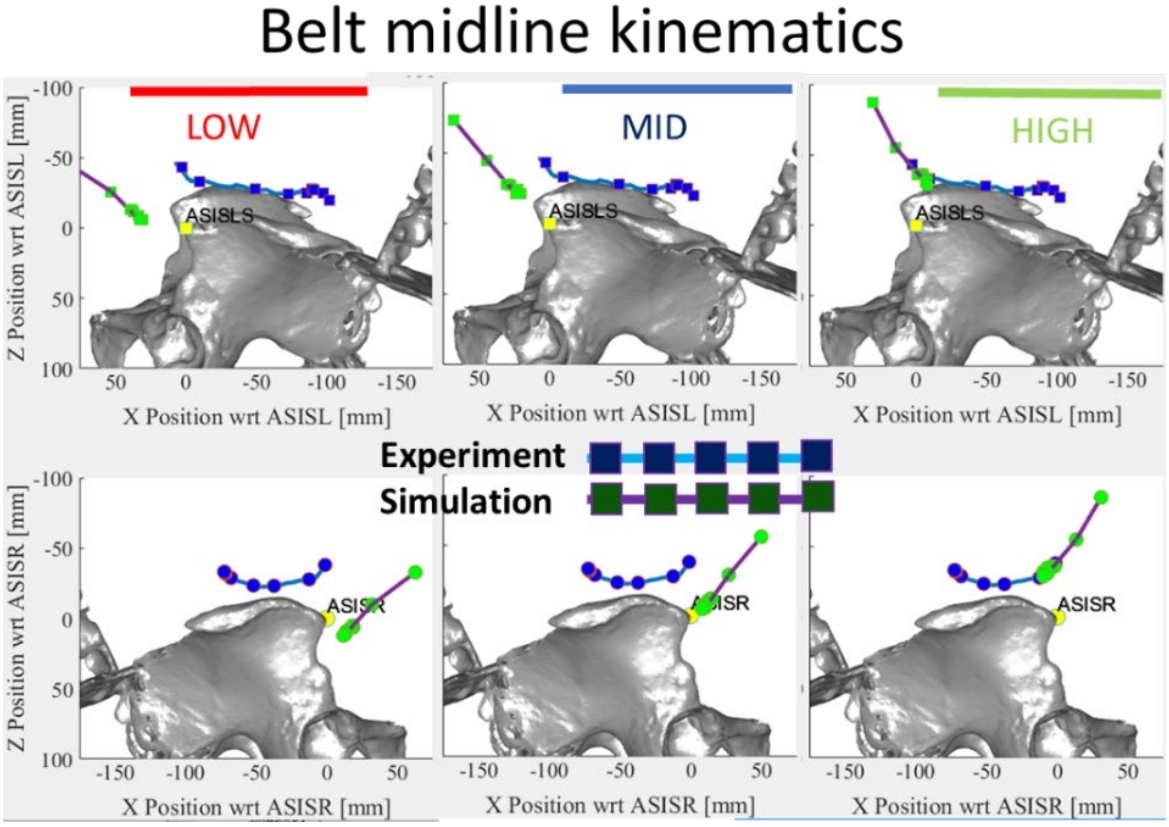

Figure 20. Belt midline kinematics of the sensitivity study of belt positioning

Simulations with the belt at either the low (red), mid (blue) or high (green) position led to similar amounts of belt displacement. Analyzing the belt kinematics (Figure 20) provided more information on the relative movement between the belt and the pelvis. The figure shows the initial belt position used in the obese FEM relative to the initial belt position from the PMHS experiment. From the three analyzed initial positions of the lap belt, one can see that only the high belt position was aligned with the belt trajectory obtained from the experiment (Figure 20). Both mid and low belt positions resulted in the belt intrusion below the ASIS. However, even though the high belt position resulted in the similar starting trajectory, it failed to replicate the abdominal intrusion observed in the PMHS test. The belt compressed the abdominal flesh and stopped at the level of the ASIS. However, in the experiment the belt engaged the top of the iliac wing, slid above the ASIS, and penetrated the abdomen.

Based on these results, the high position belt was chosen as a baseline for further studies. Additionally, it should be noted that none of the belt positions were capable of replicating flesh-pelvis shearing behavior. Specifically, the belt displacement remained aligned with pulling direction, and did not change the direction of motion once the iliac wing was encountered (Figure 20). Figure 21 shows the belt displacement vs time obtained from all three simulations.

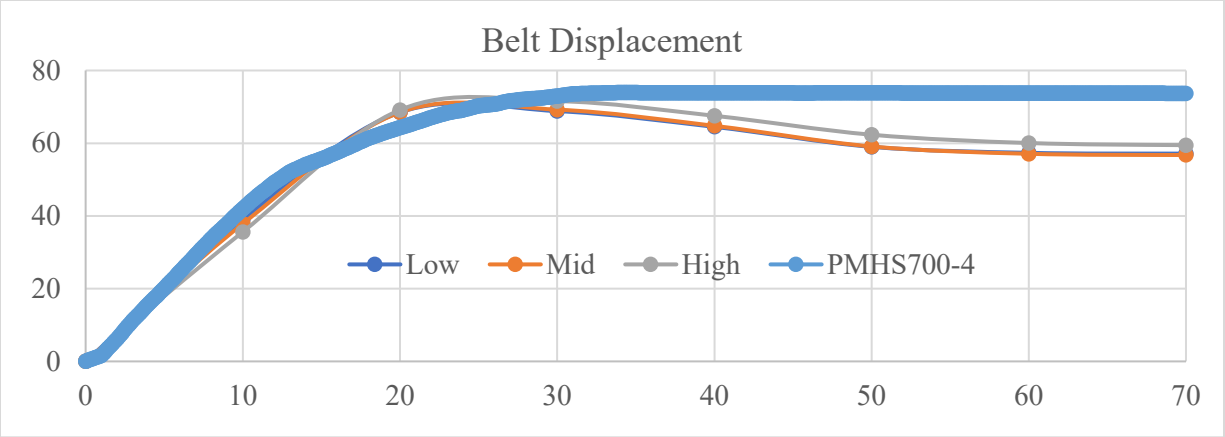

Figure 21. Belt displacement of the sensitivity study of belt positioning compared to PMHS700-4

Sensitivity of Load Limit

Since the belt in the high position showed the most promising trajectory, it was speculated that the FE simulation may not be capable of replicating the belt trajectory from the experiment due to insufficient belt pull force. It was decided that the next step should include an investigation of the loading level of the belt, and for that purpose a simulation with a doubled load level was set up. Analyzing the results showed a larger belt displacement with similar belt kinematics as the original simulation (Figure 22). Larger belt force resulted in larger abdominal flesh compression (Figure 23), however no sliding over the iliac wing into the abdomen was observed. In conclusion, the simulation with the larger belt force was not capable of replicating the flesh shearing behavior and belt sliding into the abdomen observed in the referenced PMHS test.

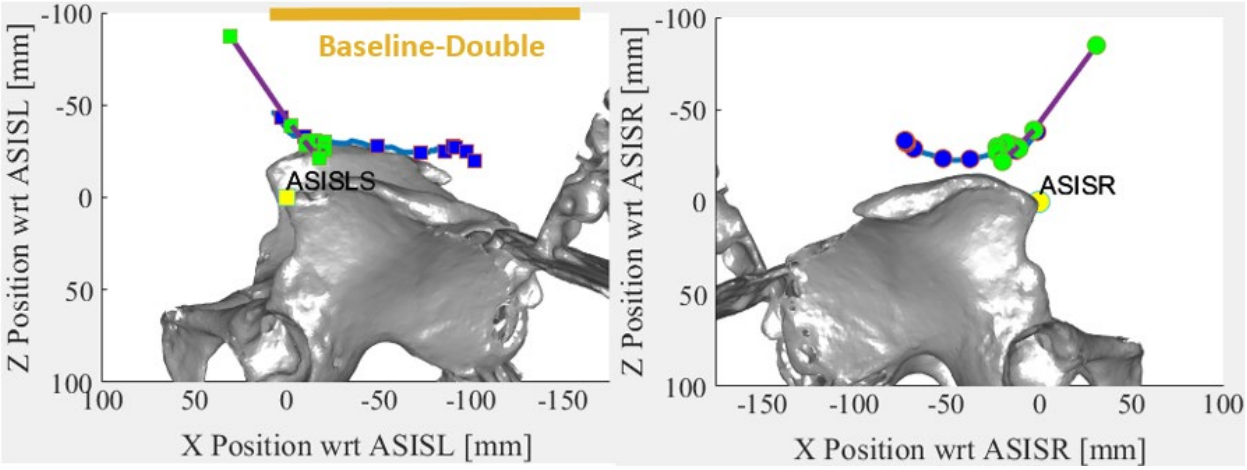

Figure 22. Belt midline kinematics of the sensitivity study of load limit

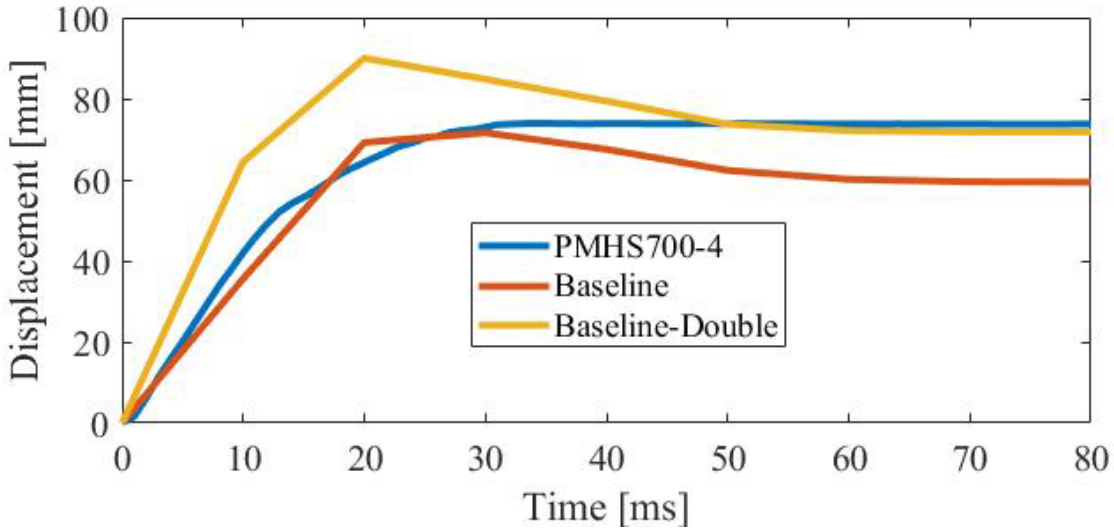

Figure 23. Belt displacement of the sensitivity study of load limit

Abdominal Organ Effects

During a progress meeting with the sponsor, a question was raised; whether the abdominal organs in the GHBMC model provide additional flesh support; that is, do they prevent the belt from penetrating into the abdomen? To address these questions from NHTSA, an GHBMC obesity model without any abdominal organs was created. A total of 37 parts were removed, including liver, spleen, gallbladder, pancreas, kidney, ureter, bladder, stomach, colon, and all relevant vessels and ligaments (Figure 24).

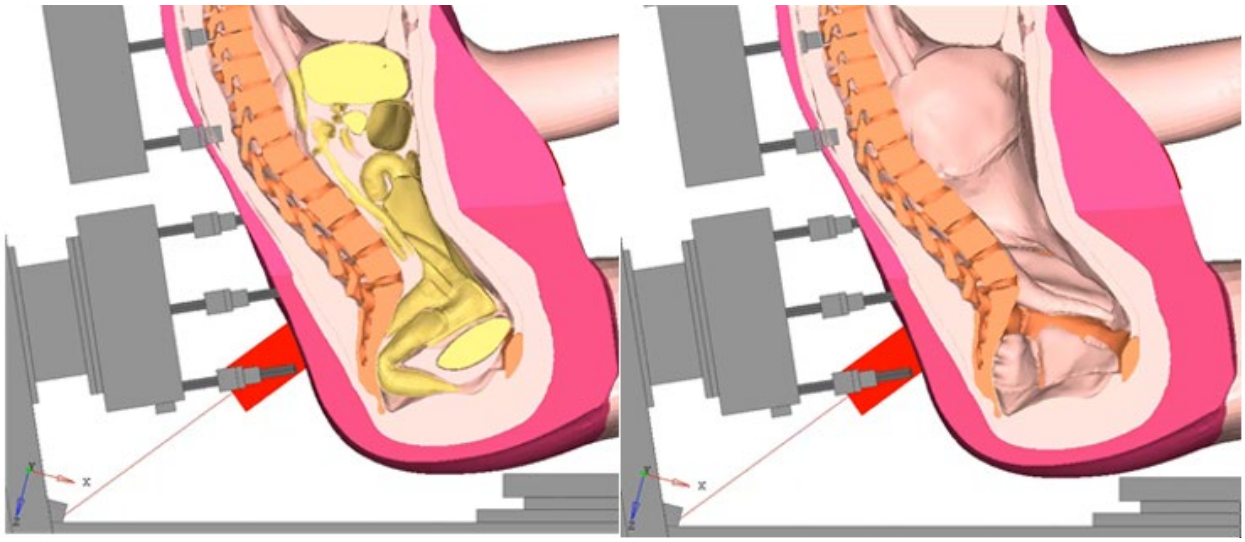

Figure 24. Comparison of the no-abdominal-organ model (right) to baseline model (left) shown in the cross-section view

In the baseline pull direction (pull down), more belt displacement was seen in the model with the abdominal organs removed than the baseline model (Figure 25). This could be explained by the fact that the abdominal organs were compressed when the belt pulled inward and compressed the abdomen, therefore providing additional compressive stiffness to the abdomen on top of the

flesh. The same conclusions can be made based on the belt kinematics plot (Figure 26), where more belt displacement was observed while the general trend of pulling direction showed no difference. The effects of the abdominal organs were also studied under extreme pulling angles, which are reported in the section on effects of extreme pulling angles.

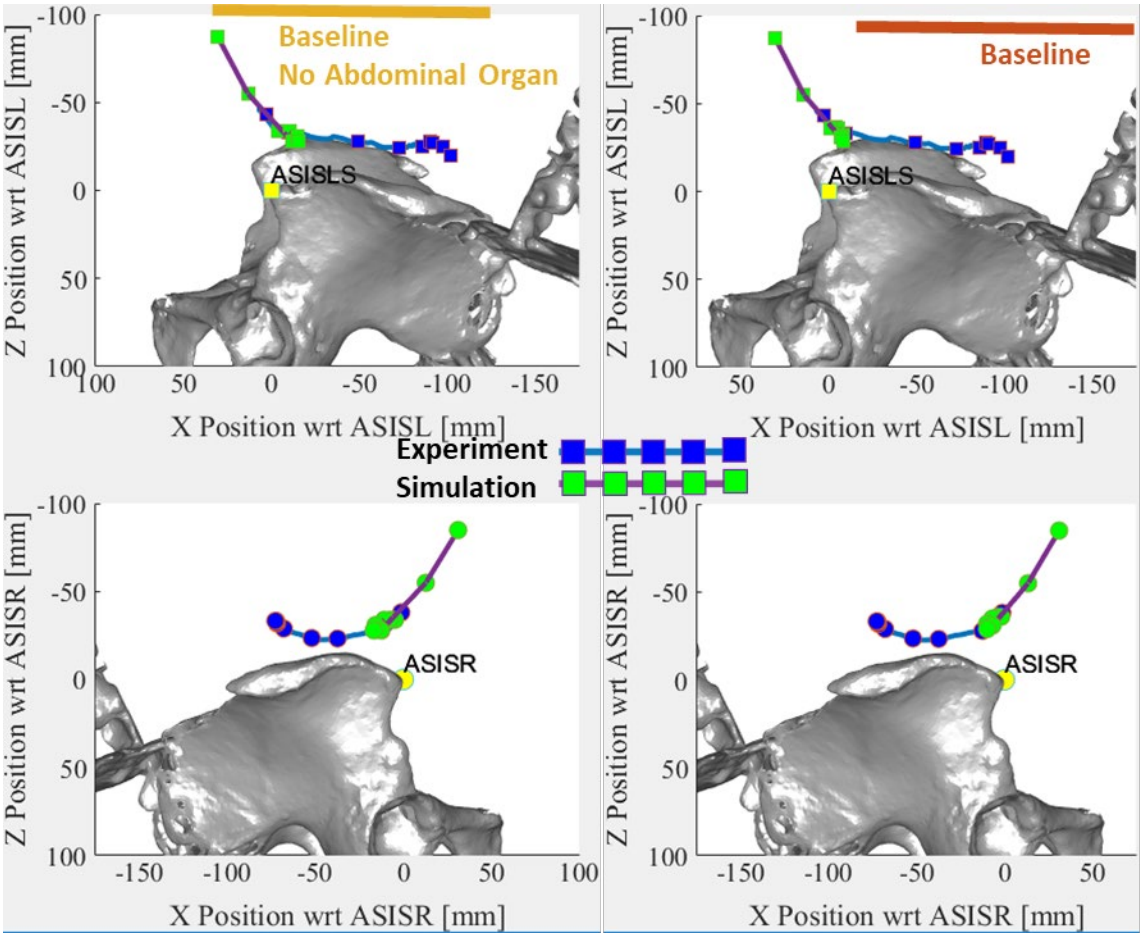

Figure 25. Belt kinematics comparison of the no-abdominal-organ model to baseline

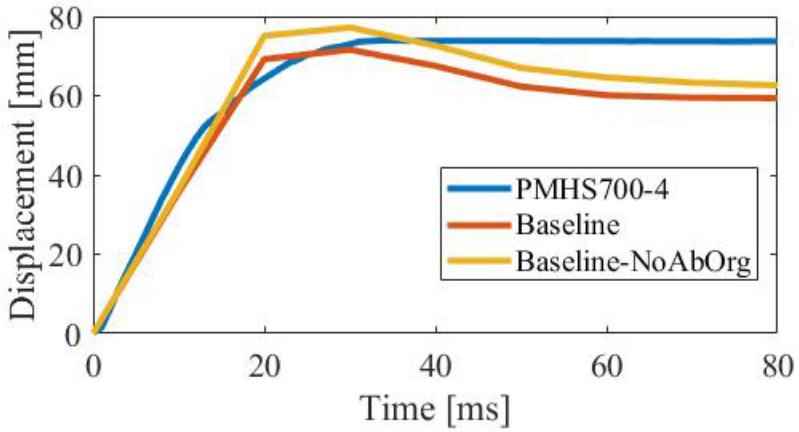

Figure 26. Belt displacement comparison of the no-abdominal-organ model to baseline

Effects on Extreme Pulling Angles

Since none of the simulations could replicate the flesh shearing and belt sliding over the pelvis, belt-pulling direction was investigated. A sensitivity study was performed for two more extreme belt-pulling directions, one pulling horizontal and one pulling up (Figure 27). Each pulling direction was simulated both on the baseline model and the no-abdominal-organ model. Including the baseline cases, a total of six simulations were performed. Side by side comparison of belt kinematics and displacements for the cases with abdominal organs are shown in Figure 28 and Figure 29, and the cases with abdominal organs removed in Figure 30 and Figure 31.

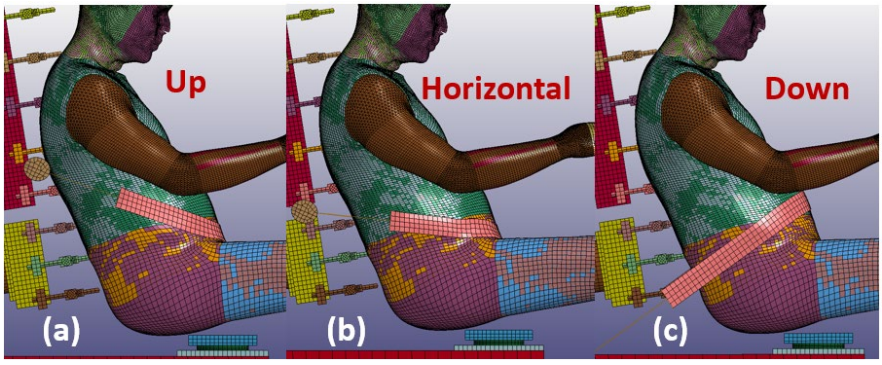

Figure 27. Three belt-pulling directions for sensitivity study (a) pulling up (b) pulling horizontal (c) pulling down (baseline)

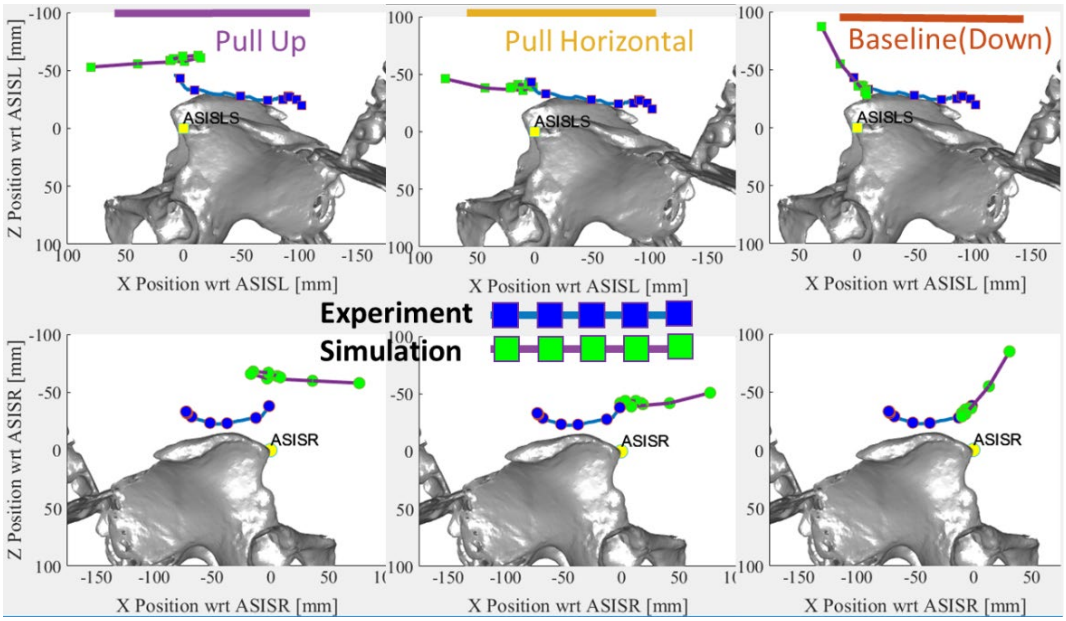

Figure 28. Belt kinematics of the sensitivity study of three belt-pulling directions on the baseline model

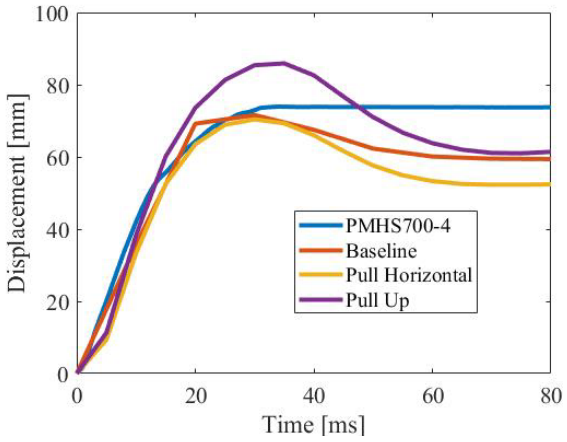

Figure 29. Belt displacements of the sensitivity study of three belt-pulling directions on the baseline model

First, the effects of belt pull direction were analyzed. For all three pulling directions in the baseline model, belts compressed the abdominal flesh. In all cases the belt motion followed the direction of belt pull without any shear movement (Figure 28). For the "Pull up" and "Pull horizontal" cases there was no pelvis engagement, and the belt motion was limited due to the increase in stiffness of the abdominal flesh with deformation. Compared with the PMHS test, the baseline and pull horizontal simulations reached a similar belt displacement level before the belt relaxed due to the release of pulling force. The pull up simulation showed a higher belt displacement (Figure 29), however the trajectory of the belt was dissimilar from the experiment (Figure 28).

Analyzing the model responses without the abdominal organ leads to similar findings (Figure 30 and Figure 31).

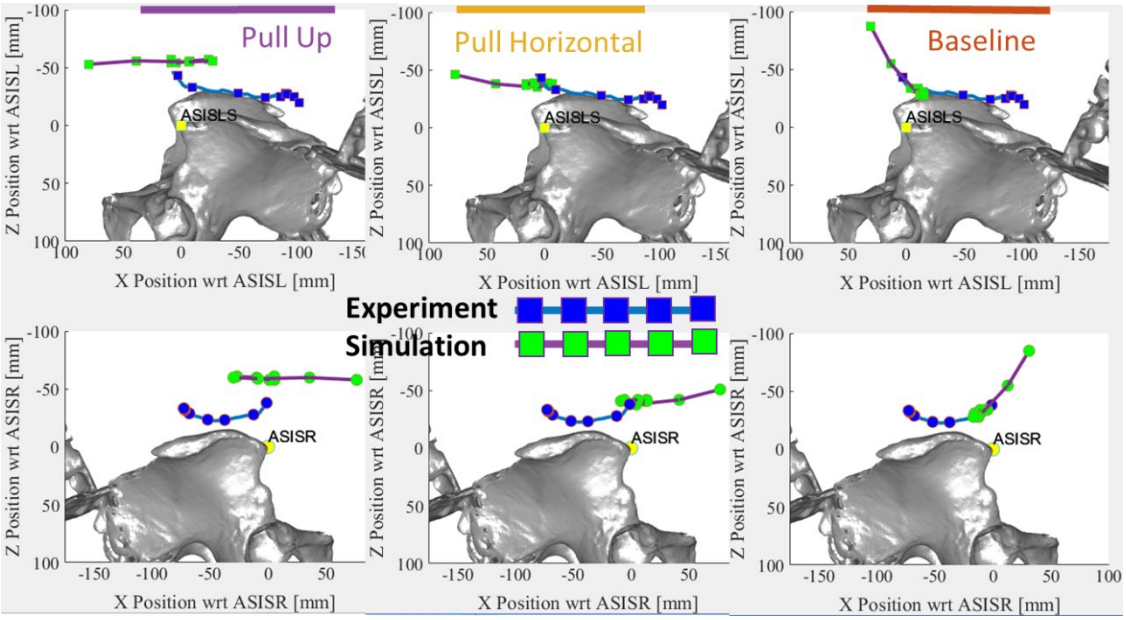

Figure 30. Belt kinematics of the sensitivity study of three belt-pulling directions on the no-abdominal-organ model

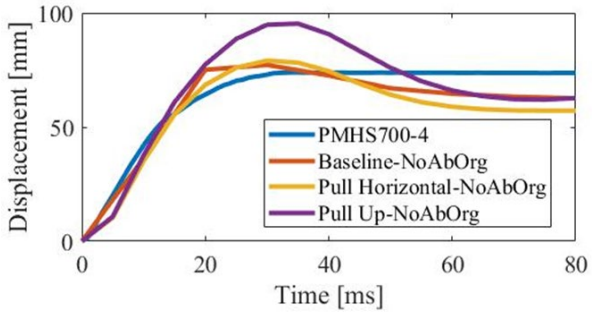

Figure 31. Belt displacements of the sensitivity study of three belt-pulling directions on the no-abdominal-organ model

The effects of removing abdominal organs from the model was investigated by comparing each of the belt pull directions individually. Results from the baseline pull direction (pull down) were reported under effects of abdominal organs (Figure 26). Similar findings were reached for both Pull-horizontal and Pull-up cases. Specifically, in both cases, more belt displacements were observed in the no-abdominal-organ models (Figure 32 and Figure 33).

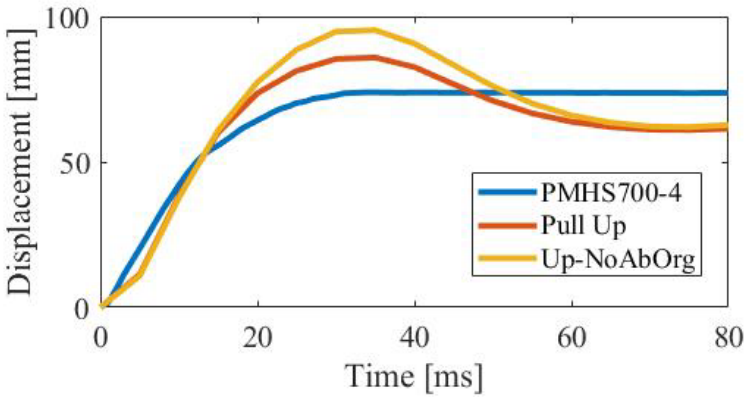

Figure 32. Belt displacements of pulling up simulation on the baseline model and the no-abdominal-organ model

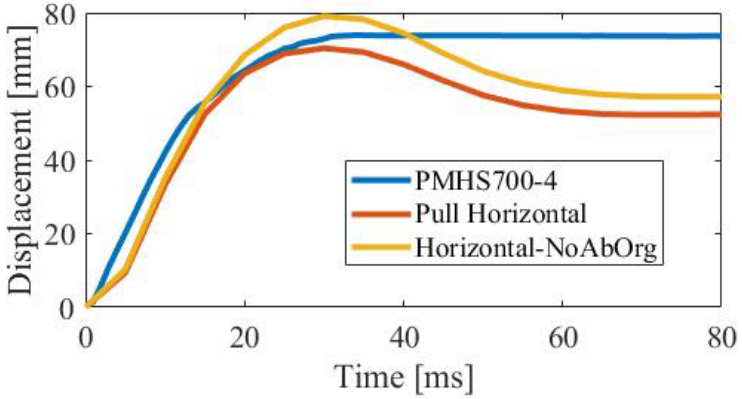

Figure 33. Belt displacements of pulling horizontal simulation on the baseline model and the no-abdominal-organ model

Abdominal Flesh Material Study

The results obtained from the GHBMC simulations performed in Task 1 showed large discrepancies from the available experimental data. It was speculated that a substantial difference in the model response was due to the stiffer shear response of the abdominal flesh. Additionally, no shearing motion of the lap belt was found on the abdominal flesh. To investigate whether this was related to the material property in the GHBMC obesity model, a literature review on subcutaneous adipose tissue properties was performed and two studies (Sommer et al., 2013; Comley & Fleck, 2012) were identified as the benchmarks of the comparison.

In the first study, Sommer et al. (2013) performed triaxial shear tests on fresh human subcutaneous adipose tissue. This data was used to evaluate the existing GHBMC adipose tissue formulation and material model. In the second study, Engelbrektsson (2011) created a material model in LS-DYNA matching the material response of a porcine subcutaneous adipose tissue tested by Comley and Fleck (2012). This material model was evaluated and compared with the current GHBMC material implementation.

Material Testing From the Literature

Sommer et al. (2013) performed triaxial shear tests on fresh human subcutaneous adipose tissue (Figure 34). A finite element simulation of a cube of GHBMC model abdominal flesh was created matching the loading and boundary conditions of the test. It was found that under the same shear strain loading, the shear stress of the GHBMC model is an order of magnitude stiffer than the tested specimen (Figure 35). It was also verified that the material model used in the GHBMC obesity model was rated insensitive.

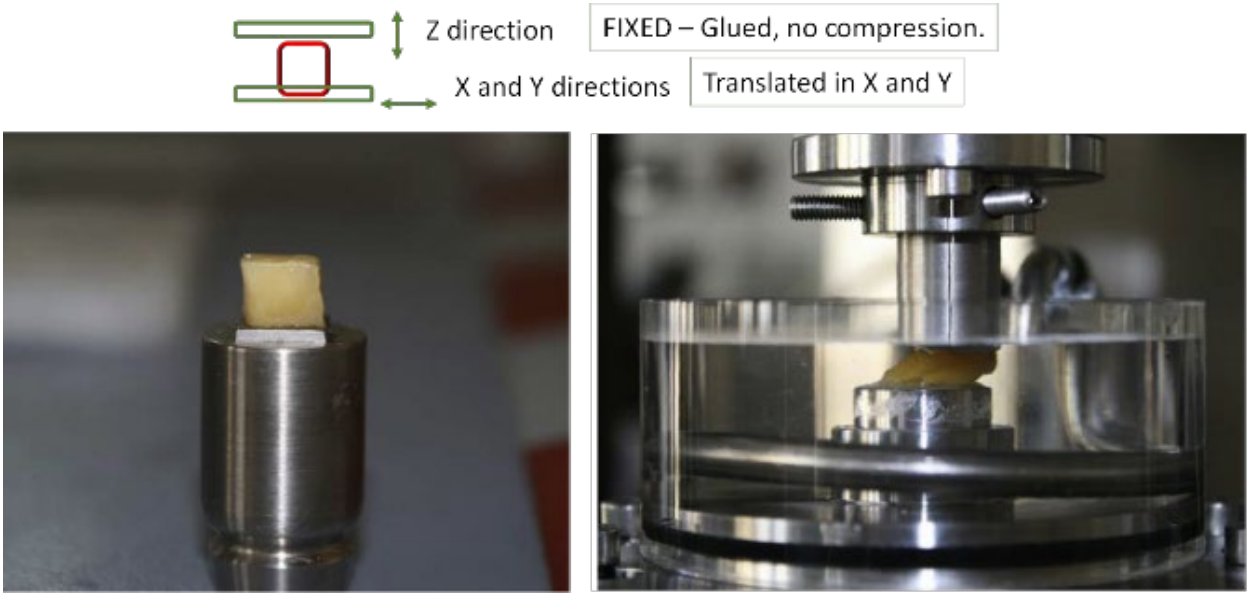

Figure 34. Test fixture adapted from Sommer et al. (2013) showing a cube of human subcutaneous adipose tissue undergoing triaxial shear tests

Engelbrektsson (2011) created a material model in LS-DYNA matching the test response of a porcine subcutaneous adipose tissue tested by Comley and Fleck (2012). An Ogden hyperelastic rubber model was used. In this material model (Engelbrektsson, 2011), subcutaneous adipose

tissue is several orders of magnitude stiffer in compression than in shear. However, the simplified rubber/foam material card used in GHBMC was not capable of representing this mechanical behavior. In the GHBMC obesity model, abdominal flesh compression stiffness and shear stiffness were related by the Poisson's ratio. The compression stiffness was defined by a uniaxial compression stress strain curve instead of a constitutive equation.

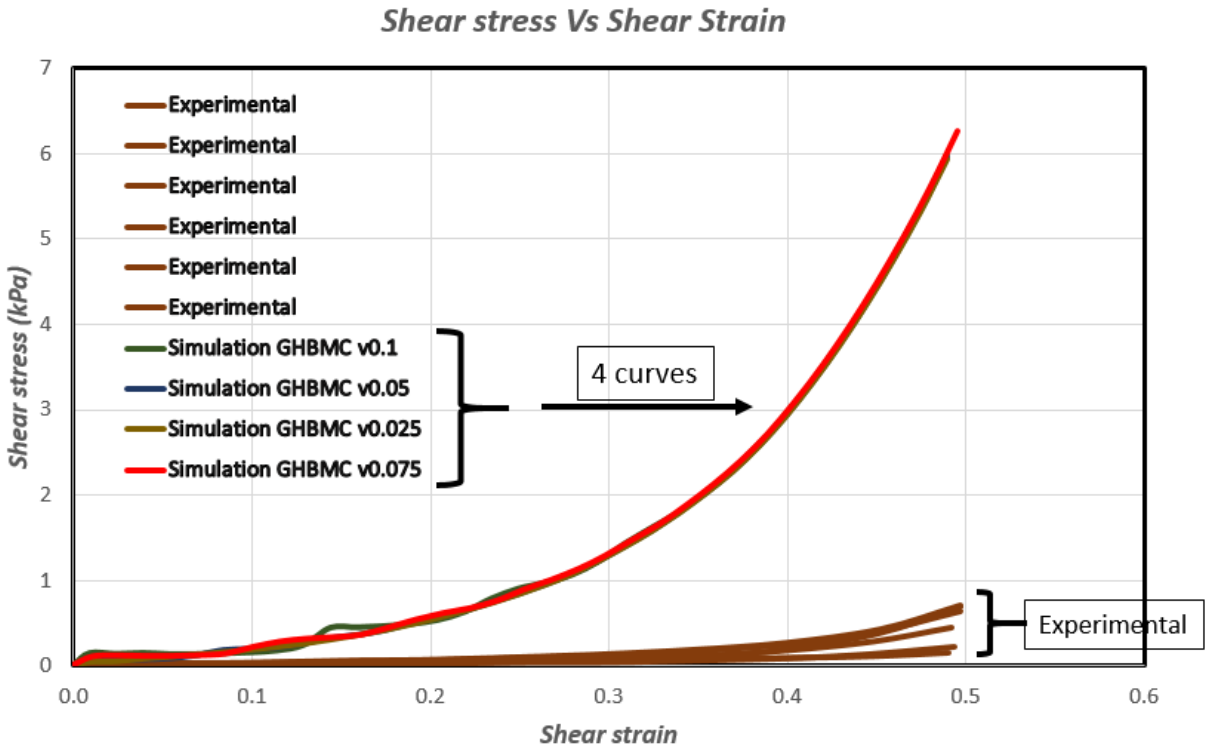

Figure 35. Comparison of the Sommer test results to the GHBMC abdominal flesh material simulation under the same loading conditions

When plotting the shear and compression stress versus strain curve, it was found that the Ogden rubber model by Engelbrektsson had a shear response at least 80 times less stiff than its compressive response while the simplified rubber/foam model (GHBMC) had a shear and compressive response on the same order of magnitude. When the lap belt was pulled towards the pelvis at an angle, one part of the force contributed to abdomen compression and the other part had a tendency to shear the tissue connected to the pelvis (Figure 36). With a shear stiffness orders of magnitude less than compression stiffness, it would be reasonable to expect that the belt would follow the path of least resistance, which would be in shear, even if the shear component of the pulling force was small. However, with similar shear and compression stiffness, as in the GHBMC model, shearing motion was not observed.

To check this assumption, the material model in GHBMC was scaled to match the shear stiffness. However, this approach also affected (decreased) the compressive stiffness, since the two are linked by the Poisson's ratio in a default GHBMC material model. Because of that, the Ogden rubber model created by Engelbrektsson was also used in comparison with the scaled GHBMC material model. Another Ogden rubber model was also created to match the original compressive stiffness of the GHBMC model and the shear stiffness of the Sommer et al. (2013) specimens.

The first material model (referred to as Sommer) was created by adding a scaling factor of 0.1 to the original GHBMC material model, effectively decreasing both the compressive and shear stiffness to 10 percent of its original level. This model matched with the upper bound in the Sommer experiments. The second model (referred to as Sommer 1/10) matched the lower bound of the Sommer experiments, scaling the original GHBMC model to its 1 percent stiffness level. The third model was directly adapted from Engelbrektsson (2011). The response of all three models is shown in Figure 37.

Figure 36. Schematics of the compression and shear components of the belt pulling force with a picture adapted from the belt pull test

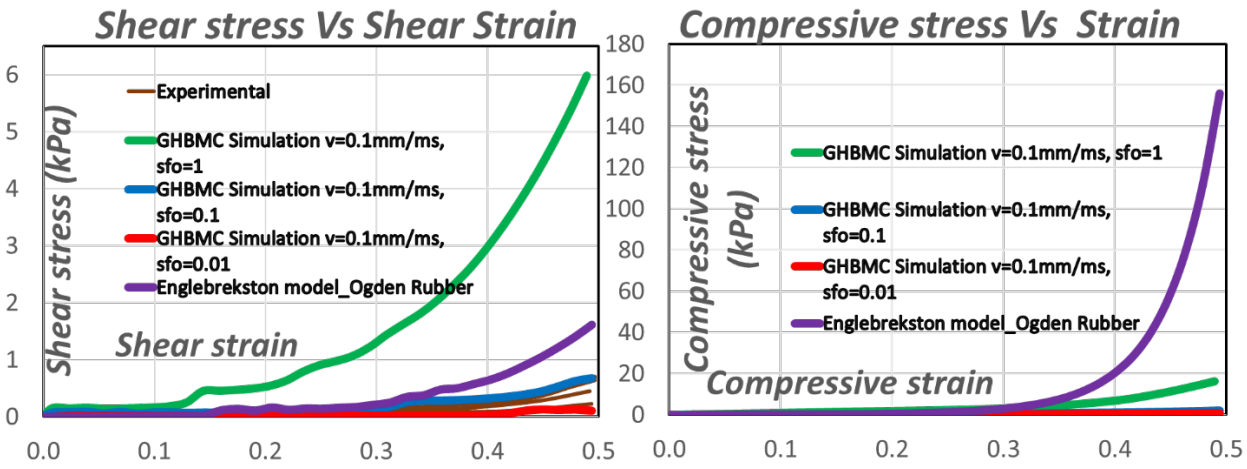

Figure 37. Shear and compressive stress strain curves from Sommer experiments, scaled GHBMC material models and Engelbrektsson Ogden hyperelastic model

Sensitivity of Material Property on Simulation Results

The baseline simulation was chosen as the reference for this sensitivity study. Loading and boundary conditions matching PMHS700-4 was adapted in all models. It was found that both Sommer and 1/10 Sommer models showed larger belt displacement than the baseline (Figure 38). This can be attributed to the decrease of compressive stiffness. Similar trends can be observed from the belt kinematics graph. In both models, the lap belt followed the original path of the experiment but penetrated more into the abdomen. It is worth noting that a 90 percent abdominal flesh stiffness decrease resulted in only 10 percent increase in belt penetration. No shearing motion was observed in both models since the relationship between shear and compression stiffness did not change (Figure 39).

The Engelbrektsson Ogden hyperelastic model showed the least amount of belt displacement since it was almost eight times stiffer in compression than the GHBMC obesity model. Interestingly, a minor change of direction of the lap belt was observed in this case (Figure 39 and Figure 40).

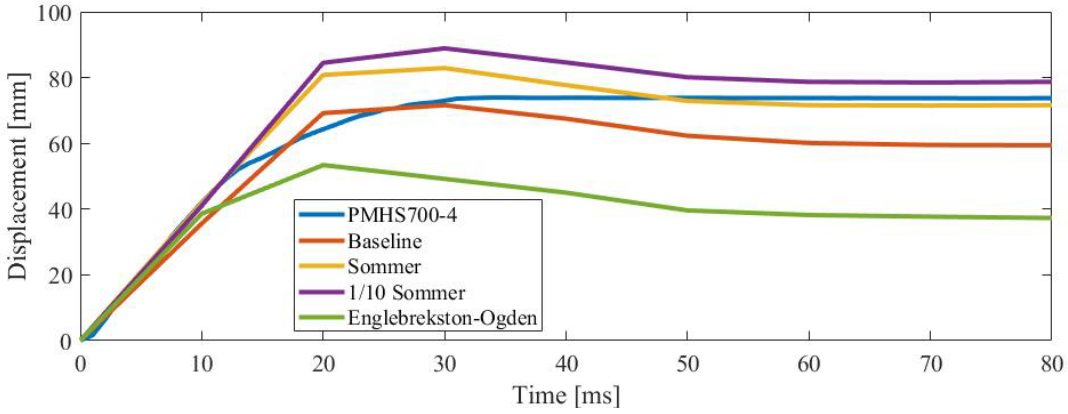

Figure 38. Belt displacements of the baseline model and models with changed material properties

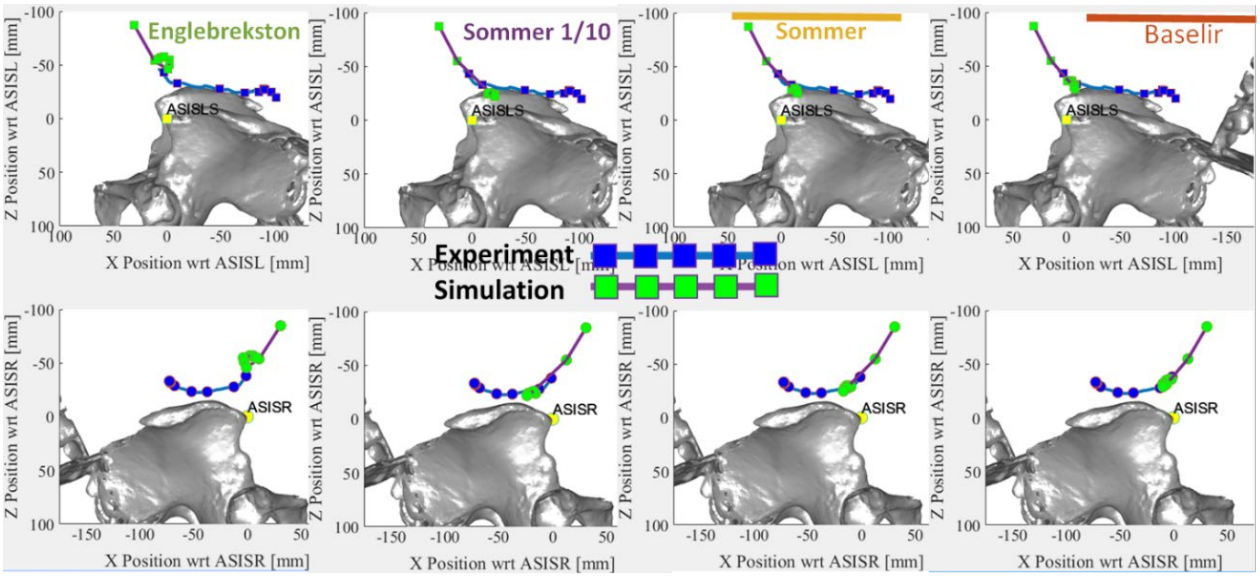

Figure 39. Belt kinematics of the baseline model and models with changed material properties

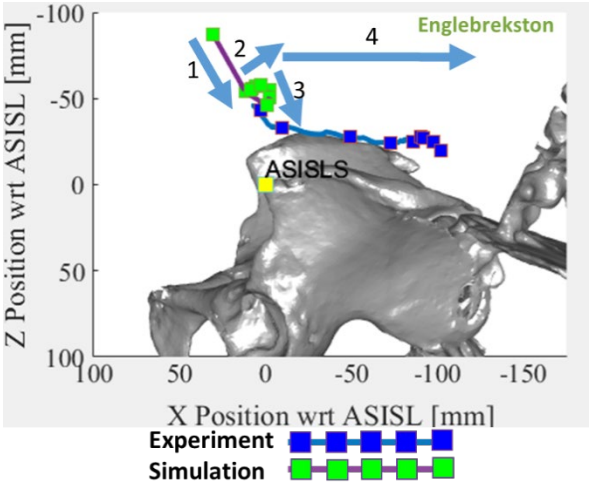

Figure 40. Actual and hypothetical lap belt movement in the simulation

Modifying material models seems to be promising, but it could prove to be a challenge for the stability of the model, under large deformation. Ideally, one would expect the belt to follow the arrows 1, 2 and 4 as shown in Figure 40. It is expected that the belt should compress the abdominal flesh until the shear resistance is overcome, which would provide a path of least resistance for the belt. The belt would then follow arrow 2, over the iliac wing and into the abdomen. The Engelbrektsson model produced a motion along arrow 1 and 2 only, which was not observed in any other material models in any other loading condition.

Page intentionally left blank.

Conclusions

The GHBMC obesity models were unable to demonstrate any belt-slip-over-pelvis kinematics that appeared in the PMHS testing. It was found that the position of the GHBMC obesity model had little to no effect on lap belt kinematics and resultant forces in the belt pull test simulations. Under the same loading and boundary conditions, the pelvis was always engaged well by the lap belt in all GHBMC positions. In all cases, increasing the lap belt load limit led to an increase in belt penetration depth, but belt displacement direction remained unchanged. Increasing the load limit could not lead to shear motion of the lap belt over the iliac wings and into the abdomen. Changing the position of the belt on the abdomen within the reasonable range could not lead to shear motion into the abdomen. Even when the lower edge of the lap belt was above the iliac wings, no shearing motion into the abdomen was observed. We conclude that pelvis engagement played a lesser role in belt engagement than the shear stiffness of the abdomen. The abdominal organs provided additional compressive stiffness, beyond what was provided by the abdominal flesh. Removing abdominal organs resulted in more belt penetration while belt kinematics remained unchanged. In extreme pulling angle cases, the direction of the belt motion aligned with the belt-pulling direction no matter how the pulling angle was changed. No shearing motion was observed. Abdominal flesh in the GHBMC obesity model appeared to be orders of magnitude stiffer in shear compared to the subcutaneous adipose tissue data. Changing material models to make shear stiffness lower did not result in improved belt motion over the pelvis.

Page intentionally left blank.

References

Comley, K., & Fleck, N. (2012). The compressive response of porcine adipose tissue from low to high strain rate. *International Journal of Impact Engineering*, *46*, 1–10.

Engelbrektsson, K. (2011). *Evaluation of material models in LS-DYNA for impact simulation of white adipose tissue* [Master thesis]. Chalmers University of Technology, Gothenburg, Sweden. www.odr.chalmers.se/server/api/core/bitstreams/341beceb-74f6-49ef-9a4f-1e2ea466638a/content

Gepner, B. D., Joodaki, H., Sun, Z., Jayathirtha, M., Kim, T., Forman, J. L. & Kerrigan, J. R. (2018, September 12-14). *Performance of the obese GHBMC models in the sled and belt pull test conditions* [Paper No. IRC-18-60]. IRCOBI Conference 2018, Athens, Greece.

Kim, T., Forman, J., & Crandall, J. (2014). *Submarining risk factors – thoracic and abdominal characterization*. Hyundai Motor Company.

Kim, J., Lee, I., Kim, T., & Kim, H. (2015, September 9-11). *Validation of abdominal characteristics under lap-belt loadings using human body model morphed to an obese female* [Paper No. IRC-15-23]. IRCOBI Conference 2015, Lyon, France.

Sommer, G., Eder, M., Kovacs, L., Pathak, H., Bonitz, L., Mueller, C., Regitnig, P.,. & Holzapfel, G. A. (2013, June). Multiaxial mechanical properties and constitutive modeling of human adipose tissue: a basis for preoperative simulations in plastic and reconstructive surgery. *Acta Biomaterialia*, *9*(11), 9036–9048.

Sun, Z., Gepner, B., & Kerrigan, J. R. (2019). *New approaches in modeling belt-flesh-pelvis interaction using obese GHBMC models*. University of Virginia Center for Applied Biomechanics.

University of Michigan Transportation Research Institute. (2017). *UMTRI morphed human models based on GHBMC M50 - O v4.4*.

DOT HS 813 540c
May 2024

U.S. Department
of Transportation

**National Highway
Traffic Safety
Administration**

16164c-050324-v3